ELSEVIER

Journal of Chromatography A, 766 (1997) 15–25

JOURNAL OF CHROMATOGRAPHY A

Effect of mobile phase composition on the binding kinetics of chiral solutes on a protein-based high-performance liquid chromatography column: Interactions of D- and L-tryptophan with immobilized human serum albumin

Ju Yang[1], David S. Hage*

Department of Chemistry, University of Nebraska-Lincoln, Lincoln, NE 68588-0304, USA

Received 23 August 1996; revised 18 November 1996; accepted 20 November 1996

Abstract

This work examined the kinetic interactions of chiral solutes on immobilized protein columns, using the binding of D- and L-tryptophan to human serum albumin as a model. Based on band-broadening studies and previous measurements of the association equilibrium constants (K_a) for this system, estimates were obtained for the dissociation and association rate constants (k_d and k_a) for D- and L-tryptophan under a variety of operating conditions. The relative importance of k_a versus k_d in creating changes in the overall binding affinity was then considered. For example, an increase in temperature from 4 to 45°C gave a large change in k_a for L-tryptophan that was due both to an increase in k_d and to a decrease in k_a, while k_a and k_d for D-tryptophan showed a parallel increase that led to a much smaller temperature dependence for K_a. Similar comparisons between k_a, k_d and K_a were performed over a range of pH values, ionic strengths and solvent polarities. It was also possible from these studies to examine the changes in enthalpy and entropy that accompanied the formation of the activated complex between human serum albumin and each solute. The results from this work were then used to illustrate the importance of kinetics and band-broadening in protein-based chiral separations, and an example was provided showing how this type of kinetic data might be used to help optimize such separations.

Keywords: Kinetic studies; Thermodynamic parameters; Enantiomer separation; Immobilized proteins; Mobile phase composition; Albumin; Tryptophan

1. Introduction

The separation of chiral molecules is an area of increasing importance in pharmaceutical testing and in the separation of biologically active compounds [1,2]. However, chiral separations also present many unique and difficult challenges. To meet these challenges, a number of techniques have been developed for chiral separations, including several based on immobilized protein supports. Examples of proteins that have been used for this purpose include α_1-acid glycoprotein, serum albumin, ovomucoid, avidin and cellulase [1–3].

Although there is now a reasonable amount of

*Corresponding author.

[1]Current address: Environmental Chemistry, Rhone-Poulenc Ag Company, Research Triangle Park, NC 27709, USA

PII S0021-9673(96)01040-0

information regarding what types of mobile phases should be used with these protein supports for chiral separations (e.g., see Ref. [2]), much less is known about the actual nature of these separation processes. A number of recent reports have examined the thermodynamic properties and binding mechanisms involved in the interactions of some model compounds with proteins such as human serum albumin [4–6] or turkey ovomucoid [7]. However, there is still little data available on the kinetics of these interactions [6]. Such data would be useful in the design of new protein-based separations, since protein supports tend to have lower efficiencies than more traditional types of chromatographic columns [3,6].

This work will examine the kinetics involved during the interactions of some model solutes with the protein human serum albumin (HSA). HSA is a 66.5-kDa protein that is responsible for the transport of a wide variety of biological and pharmaceutical compounds in blood [8–12]. The interaction of these compounds with HSA is believed to occur at a series of well-defined binding sites on the surface of the protein [11,12], with the strength and number of sites to which a given molecule binds varying from one solute to the next or even between different chiral forms of the same compound [11]. This ability to provide chiral discrimination, plus the inherent biological importance of HSA, have made this protein attractive for use as a model in studies examining some of the mechanisms of protein-based chiral separations and stereoselective solute–protein interactions [4–6,13].

The D- and L-enantiomers of tryptophan have received particular attention in recent studies with HSA columns because of their relatively well-characterized binding properties with this protein [4,14,15]. For example, L-tryptophan has a single binding region on HSA that is known to be located at the indole–benzodiazepine site of this protein [12,16]. Crystallographic studies have identified this site as being in the IIIA subdomain of HSA [17] and the amino acid residues that make up this site are fairly well-known [16–19]. D-Tryptophan is also believed to bind at a single site on HSA, but has a much weaker affinity than L-tryptophan [13,20,21] and interacts at a separate binding region [13]. Although the exact location of the D-tryptophan site is not known, D-tryptophan does have some indirect interactions with the warfarin–azapropazone site of HSA [13].

In previous work, frontal analysis and zonal elution methods have been used to examine the thermodynamic processes involved in the binding of D- and L-tryptophan to immobilized HSA columns under various mobile phase conditions [4,13]. This study will examine how mobile phase composition affects the kinetics between these solutes and HSA. This will be done by estimating the association and dissociation rate constants for this system through the use of plate height measurements, as performed for mobile phases at a variety of pH values, temperatures, ionic strengths and solvent polarities. The resulting data should provide valuable clues as to how mobile phase composition affects the rate of solute–protein interactions and their corresponding band-broadening processes. Such data should also be useful in the design or optimization of new chiral separations based on HSA or other types of immobilized proteins.

2. Theory

The kinetics of D- and L-tryptophan interactions with immobilized HSA were examined through the use of plate height measurements. This was performed in the same manner as described in previous work that examined the binding of *R*- and *S*-warfarin with HSA [6]. This approach involved a detailed examination of the various band-broadening processes that occurred on the HSA column. For example, the total measured plate height (H_{tot}) for such a column can be expressed as the following sum of individual plate height terms

$$H_{tot} = H_m + H_L + H_{sm} + H_s + H_{ec} \quad (1)$$

where the items on the right-hand side of Eq. (1) represent the contributions due to mobile phase mass transfer (H_m), longitudinal diffusion (H_L), stagnant mobile phase mass transfer (H_{sm}), stationary phase mass transfer (H_s) and extra-column band-broadening (H_{ec}) [22].

When evaluating the terms in Eq. (1), H_{ec} can be

determined by measuring the plate height for the solute as it is injected onto the high-performance liquid chromatography (HPLC) system when all components except the column are present. In addition, it is generally possible to ignore the term H_L since this is usually much smaller than the other plate height terms in Eq. (1) [6,22,23]. Another useful assumption is that H_m is independent of flow-rate or has only a small flow-rate dependence under the typical operating conditions used in HPLC. This allows H_m to be estimated from the intercepts of plots made for H_{tot} versus linear velocity [22,23], as will be shown later in Eqs. (4,5).

The term in Eq. (1) that was of most interest in this study was the contribution due to stationary phase mass transfer (H_s). H_s can be described by the following equation for a column that contains a stationary phase with a fixed number of ligand sites, such as the immobilized HSA support used in this work [22]:

$$H_s = \frac{2uk'}{k_d(1+k')^2} \tag{2}$$

In Eq. (2), u is the linear velocity of mobile phase in the column, k' is the capacity factor of the solute and k_d is the apparent rate constant for the dissociation of solute from the immobilized ligand. It is assumed in Eq. (2) that either solute–ligand binding occurs at a single type of site in the column or that the net rate of these interactions can be described by a single set of rate constants. It is also assumed that linear elution conditions are present (i.e., the amount of injected solute is small versus the amount of immobilized ligand in the column) [22]. According to Eq. (2), a plot of H_s versus $[uk'/(1+k')^2]$ should give a straight line with a slope of $(2/k_d)$ and an intercept of zero, thus providing the value of k_d for the solute–ligand interactions. If the association equilibrium constant (K_a) for solute–ligand binding is also known, then it is possible to calculate the corresponding apparent association rate constant (k_a) by using the relationship $K_a = (k_a/k_d)$ [6].

To determine the value of H_s from H_{tot}, the plate height contribution due to stagnant mobile phase mass transfer (H_{sm}) must also be estimated. The value of H_{sm} for a porous, spherical support can be described by the expression [24]

$$H_{sm} = \frac{2uV_p[1+(V_mk'/V_p)]^2}{k_{-1}V_m(1+k')^2} \tag{3}$$

where V_p is the volume of mobile phase within the pores of the support (i.e., the volume of stagnant mobile phase), V_m is the total volume of mobile phase in the column (i.e., the column void volume) and k_{-1} is a combination of geometrical and physical factors (e.g., particle size and diffusion coefficients) that describe the mass transfer of solute from the inside to the outside of the porous support [25]. One way that H_{sm} can be determined is by combining Eqs. (1–3) to give the following relationship, where the total plate height after correction for extra-column band-broadening is represented by $(H_{tot}-H_{ec})$:

$$(H_{tot}-H_{ec}) = H_m + \frac{2uV_p[1+(V_mk'/V_p)]^2}{k_{-1}V_m(1+k')^2} + \frac{2uk'}{k_d(1+k')^2} \tag{4}$$

A simpler version of Eq. (4) is obtained if band-broadening studies are performed with a non-retained solute (i.e., $k'=0$), in which case, the relationship in Eq. (5) is obtained.

$$(H_{tot}-H_{ec}) = H_m + \frac{2uV_p}{k_{-1}V_m} \tag{5}$$

This new expression predicts that a plot of $(H_{tot}-H_{ec})$ versus u for a non-retained solute will give a linear relationship with a slope of $(2V_p/k_{-1}V_m)$ and an intercept of H_m. By using the resulting slope and independent estimates of V_m and V_p, the value of k_{-1} for the given solute and support can be obtained. These data can then be used along with Eq. (3) to estimate the value of H_{sm} when the solute is injected onto the same support but in the presence of an immobilized ligand. By subtracting this term (as well as H_m, H_{ec}, etc.) from H_{tot}, the portion that remains should be equal to the value of H_s for the solute. This can then be further analyzed, as shown earlier with Eq. (2), to obtain the value of k_d for the solute and immobilized ligand.

Many of the parameters that make up the plate height terms in Eqs. (2–5) are temperature-dependent (e.g., k_d, k' and k_{-1}). This means that each plate height term should be determined under the same

temperature conditions in order to obtain accurate estimates of k_d and k_a. By using this approach to determine k_d and k_a over a range of temperatures, information can also be obtained on the energetics of solute–ligand binding. For example, according to the activated complex theory, the second order association rate constant for solute–ligand binding (k_a) can be related to the absolute temperature (T) through the following equation [26].

$$\ln(k_a/T) = \ln(\kappa R/Nh) - (\Delta H^{\ddagger}/RT) + (\Delta S^{\ddagger}/R) \quad (6)$$

where R is the ideal gas law constant, N is Avogadro's number, h is Planck's constant and κ is the transmission coefficient for the reaction (usually taken as being equal to one). The term $\Delta H^{\ddagger}$ is the change in enthalpy during the formation of the activated complex from the initial reactants and $\Delta S^{\ddagger}$ is the associated change in entropy for this process. Eq. (6) predicts that a plot of $\ln(k_a/T)$ versus $1/T$ will yield a linear relationship with a slope of $-\Delta H^{\ddagger}/R$ and an intercept of $[\ln(\kappa R/N h)+(\Delta S^{\ddagger}/R)]$. From the values of $\Delta H^{\ddagger}$ and $\Delta S^{\ddagger}$ that are determined from the slope and intercept, the change in free energy in going from the initial reactants to the activated complex ($\Delta G^{\ddagger}$) can also be calculated, as discussed previously [6].

3. Experimental

3.1. Reagents

The D-tryptophan, L-tryptophan and HSA (Cohn fraction V, 99% globulin-free) were purchased from Sigma (St. Louis, MO, USA). The Nucleosil Si-300 (10 μm particle diameter, 300 Å pore size) was from Alltech (Deerfield, IL, USA). The reagents for the bicinchoninic acid (BCA) protein assay were obtained from Pierce (Rockford, IL, USA). The HPLC-grade 1-propanol and uracil were from Aldrich (Milwaukee, WI, USA). All other chemicals used were of the purest grade available. All solutions were prepared with water from a Nanopure water system (Barnstead, Dubuque, IA, USA).

3.2. Apparatus

The chromatographic system consisted of one CM3000 isocratic pump, one CM4000 gradient pump and one SM3100 UV–Vis variable wavelength absorbance detector from LDC/Milton Roy (Riviera Beach, FL, USA). Samples were injected using a Rheodyne 7012 valve (Cotati, CA, USA) equipped with a PhaseSep event marker (Phase Separations, Queensferry, UK) and a 20-μl injection loop. An LDC/Milton Roy Chromlink interface and LCAdvantage software were used for data collection. Chromatographic data were processed using programs written in QuickBASIC (Redmond, WA, USA) with double-precision logic. An Isotemp 9100 circulating waterbath (Fisher Scientific, Pittsburgh, PA, USA) was used for temperature control of both the column and the mobile phases. All columns were packed using an Alltech HPLC column slurry packer.

3.3. Methods

The diol-bonded silica and immobilized HSA silica supports were prepared from Nucleosil Si-300, as described previously [4,5]. The initial coverage of the diol-bonded silica was 25±6 μmol (±1 S.D.) diol groups per gram of silica, as determined in duplicate by an iodometric titration. After the immobilized HSA silica had been prepared, it was washed and stored in 0.10 M phosphate buffer (pH 7.0) and kept at 4°C until use. A small portion of the HSA support was further washed with deionized water, dried under reduced pressure and analyzed by using a BCA protein assay [27]. The BCA assay was performed using BSA as the standard and diol-bonded silica as the blank. Based on duplicate assays, the amount of immobilized HSA was determined to be 500±7 nmol (±1 S.D.) HSA per gram of silica.

3.4. Chromatography

The immobilized HSA and diol-bonded silica supports were downward slurry-packed into two separate 100.0×4.1 mm I.D. stainless steel columns at a pressure of $400 \cdot 10^5$ Pa using 0.10 M phosphate buffer (pH 7.0) as the packing solvent. Both columns were enclosed in water jackets for temperature control. All studies, except those examining the temperature dependence of tryptophan–HSA binding, were performed at 25±0.1°C. The mobile

phases used in this work were filtered prior to use by passing them through 0.45 μm cellulose acetate or nylon filters. All mobile phases were degassed under vacuum for at least 10 min before use on the HPLC system. Elution of the D- and L-tryptophan was monitored at 290 nm.

The association equilibrium constants given in this work were measured by frontal analysis on the immobilized HSA column, as described previously [13]. The plate height and kinetic studies were performed in a similar fashion to that described in Ref. [6] and were carried out at flow-rates ranging from 0.50 to 1.50 ml/min. The D- and L-tryptophan solutions were freshly prepared for each experiment by dissolving up to $1 \cdot 10^{-5}$ *M* of the appropriate enantiomer into the buffer being used as the mobile phase [4]. Three injections of sample were made onto both the HSA and diol-bonded silica columns under each set of mobile phase conditions. The value of the column's void volume (V_m) was determined from the data collected on the diol-bonded silica column; the column pore volume (V_p) was determined by using the measured value for V_m and information on the relative pore volume and packing density of the Nucleosil Si-300 support, as provided by the manufacturer. The retention times and variance of the D- and L-tryptophan peaks were calculated by using moments analysis and the modified $B/A_{0.1}$ method, respectively [28,29]. Corrections for the extra-column volume and extra-column band-broadening were made by making injections of D- or L-tryptophan onto the chromatographic system with no column present [6].

The stability of the HSA column was checked periodically by making injections of D- and L-tryptophan under a set of standard conditions (i.e., pH 7.0, 0.05 *M* phosphate buffer applied at 25°C at a flow-rate of 1.0 ml/min) [13]. No detectable changes were noted under these conditions for either the elution times or widths of the tryptophan peaks throughout the course of this study (i.e., a period of about 30 months or 1000 sample injections).

4. Results and discussion

Van Deemter-type plots of total plate height versus linear velocity were initially used to characterize the band-broadening of D- and L-tryptophan on immobilized HSA. The general behavior of such plots is shown in Fig. 1a, using data obtained for the binding of D-tryptophan to HSA at several different mobile phase pH values as an example. Under the flow-rate conditions used in this work, all of the graphs in Fig. 1a gave a linear relationship between H_{tot} and linear velocity, as predicted by the model used in Eq. (4). The correlation coefficients for these plots ranged from 0.9774 to 0.9989 over data measured in triplicate at five flow-rates. For the other mobile phase conditions examined in this study, similar graphs were obtained for D-tryptophan, with correlation coefficients of between 0.9415 and 0.9999 for data at five flow-rates covering approximately the same range of conditions as shown in Fig. 1a. The same type of linear behavior was observed for L-tryptophan under equivalent flow-rate and mobile

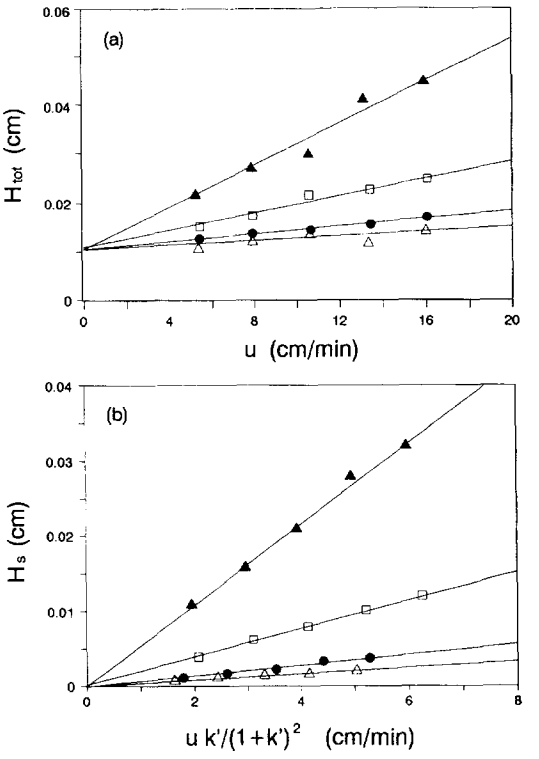

Fig. 1. Typical plots of (a) total plate height and (b) plate height contribution due to stationary phase mass transfer versus linear velocity or $[u\ k'/(1+k')^2]$ for D-tryptophan injected onto an immobilized HSA column at 25°C and mobile phase pH values of 4.0 (△), 5.0 (●), 6.0 (□) or 7.0 (▲).

phase conditions, with correlation coefficients of 0.9623 to 0.9999 being measured.

Based on studies performed with D- and L-tryptophan on a diol-bonded silica column (i.e., where $k'=0$ for these compounds) and on a chromatographic system in the absence on any column, it was possible to estimate the contributions of the plate height terms H_{ec}, H_{sm} and H_m to plots like those in Fig. 1a, as performed according to procedures discussed earlier in Section 2. By taking the difference between these terms and H_{tot}, it was then possible to determine the plate height contribution due to stationary phase mass transfer (H_s). Once values of H_s had been obtained for each set of retention, flow-rate and mobile phase conditions, plots of H_s versus $[u\,k'/(1+k')^2]$ were made according to Eq. (2). Fig. 1b shows some typical examples of such graphs, which were generated based on the same data as used for the van Deemter-type plots in Fig. 1a. In each case, a linear relationship between H_s and $[u\,k'/(1+k')^2]$ was obtained with a positive slope and intercept at or near zero, as predicted by Eq. (2). The correlation coefficients for such plots under all tested mobile phase conditions ranged from 0.9842 to 0.9994 for D-tryptophan and 0.9898 to 0.9998 for L-tryptophan. From the slopes of these plots it was possible to estimate the value of the dissociation rate constant (k_d). By combining these results with association equilibrium constants (K_a) that were previously measured for D- and L-tryptophan on the same type of HSA column [13], the association rate constant (k_a) under each set of conditions could also be determined. The k_d, k_a and K_a values that were obtained by this process are summarized in Figs. 2–6. The precision of the rate constants varied from ±7–35% (1 R.S.D.), with a mean precision of about ±15% for k_a and k_d. The K_a values also had precisions in the range of ±8–35%, as reported earlier [13].

The temperature of the chromatographic system was one item that was examined for its effects on the band-broadening of D/L-tryptophan on an immobilized HSA column. The rate constants obtained over the range from 4 to 45°C are given in Fig. 2. Also included in Fig. 2 is a graph showing the known association equilibrium constants for D- and L-tryptophan at each temperature, as previously measured on the same HSA column by frontal analysis

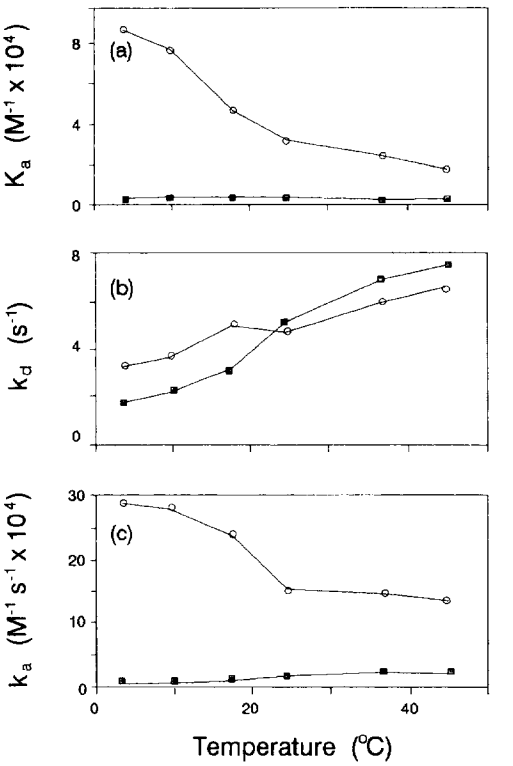

Fig. 2. Effect of system temperature on the (a) association equilibrium constants, (b) dissociation rate constants and (c) association rate constants for D-tryptophan (■) and L-tryptophan (○) on an immobilized HSA column.

[13]. The values for k_a that were noted in this graph are similar to those reported for *R*- and *S*-warfarin with immobilized HSA [6], but k_d was an order of magnitude larger for the tryptophan–HSA system. In addition, the rate constants measured in this study were similar to those observed during the binding of other solutes (e.g., L-triiodothyronine, bilirubin and salicylazosulfapyridine) with HSA or bovine serum albumin in solution under comparable conditions [30–32].

As noted previously [13], the association equilibrium constant for L-tryptophan with immobilized HSA decreases by over four-fold in going from 4 to 45°C, but a much smaller change in K_a is noted for D-tryptophan under the same conditions. As indicated in Fig. 2, the relatively large change in K_a for L-tryptophan was the result of both a two-fold increase in k_d (i.e., faster dissociation at higher temperatures) and about a 55% decrease in k_a (i.e.,

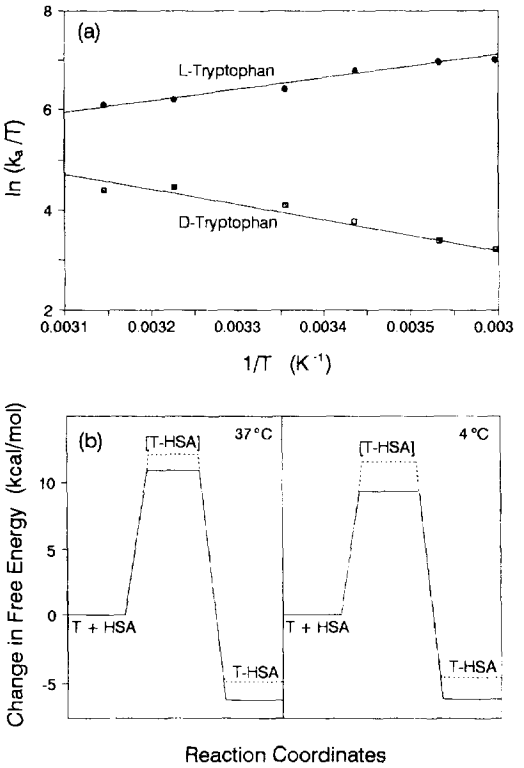

Fig. 3. (a) Change in ln (k_a/T) versus $1/T$ for D-tryptophan (■) and L-tryptophan (●) on an immobilized HSA column and (b) energy diagrams for the binding of D-tryptophan (- - -) and L-tryptophan (—) to immobilized HSA. The best-fit parameters for the plots in (a) are given in the text. In (b), the terms T+HSA, [T–HSA] and T–HSA represent the initial reactants, the activated complex and the final tryptophan–HSA complex, respectively.

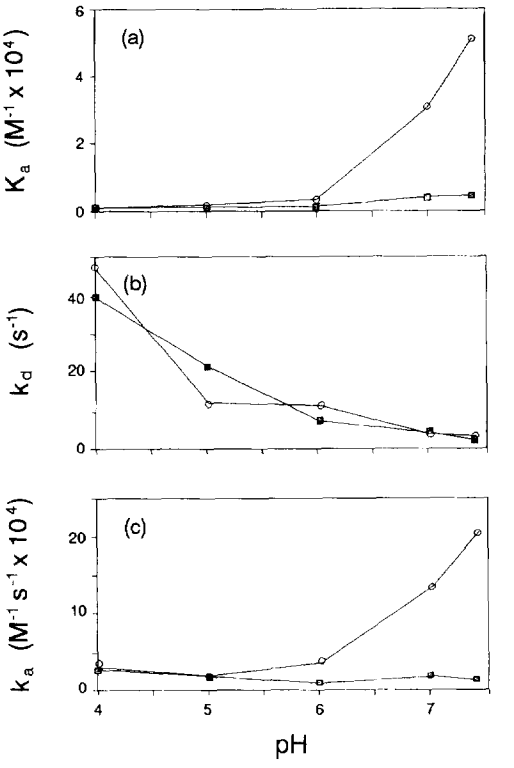

Fig. 4. Effect of mobile phase pH on the (a) association equilibrium constants, (b) dissociation rate constants and (c) association rate constants for D-tryptophan (■) and L-tryptophan (○) on an immobilized HSA column.

slower association). For D-tryptophan, much different behavior was noted in that k_a and k_d showed a parallel increase as the temperature was raised (i.e., over a four-fold increase in k_d and a 3.5-fold increase in k_a in going from 4 to 45°C). It was because of this parallel change (i.e., an increase in both association and dissociation rates with temperature) that the net value of K_a for D-tryptophan had a much smaller temperature dependence than that for the L-enantiomer.

The temperature dependence of the kinetics for D- and L-tryptophan–HSA binding was examined in more detail by replotting the rate constant data in Fig. 2 according to Eq. (6). The resulting graphs of ln (k_a/T) versus $1/T$ are shown in Fig. 3a. The graphs for both D- and L-tryptophan were linear over the entire temperature range studied. The correlation coefficients were 0.9466 and 0.9634 ($n=6$) for D- and L-tryptophan, respectively. The corresponding best-fit slopes were -2800 ± 500 (1 S.D.) and 2200 ± 300; the best-fit intercepts were 13.1 ± 0.2 and -0.9 ± 0.1. The linearity of all of these plots indicated that there was good agreement between the experimental data and the equations used in this work to describe the kinetics of tryptophan–HSA binding. Although the positive slope observed for the L-tryptophan plot is somewhat unusual, this could be produced by having a transition complex whose formation is favored by enthalpy but highly disfavored by entropy, as discussed in the next paragraph. From the slopes and intercepts of Fig. 3a it was possible to determine values for the changes in enthalpy ($\Delta H^{\ddagger}$) and entropy ($\Delta S^{\ddagger}$) in going from the initial reactants to the activated complex between D- or L-tryptophan and HSA (see Table 1). Based on

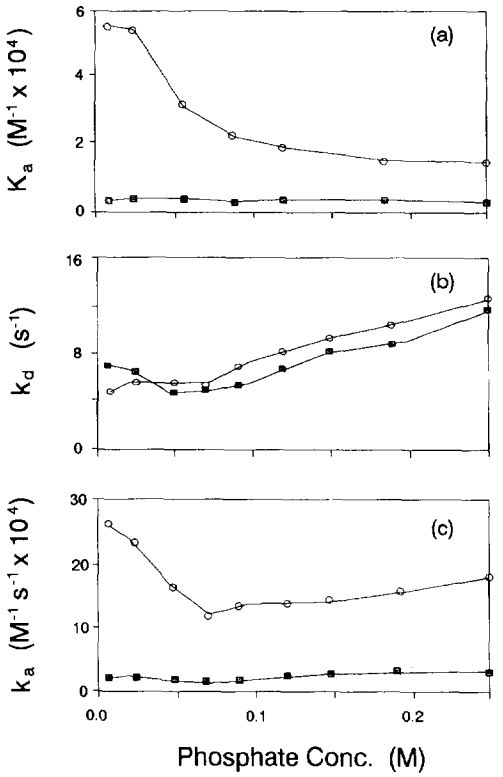

Fig. 5. Effect of mobile phase ionic strength on the (a) association equilibrium constants, (b) dissociation rate constants and (c) association rate constants for D-tryptophan (■) and L-tryptophan (○) on an immobilized HSA column.

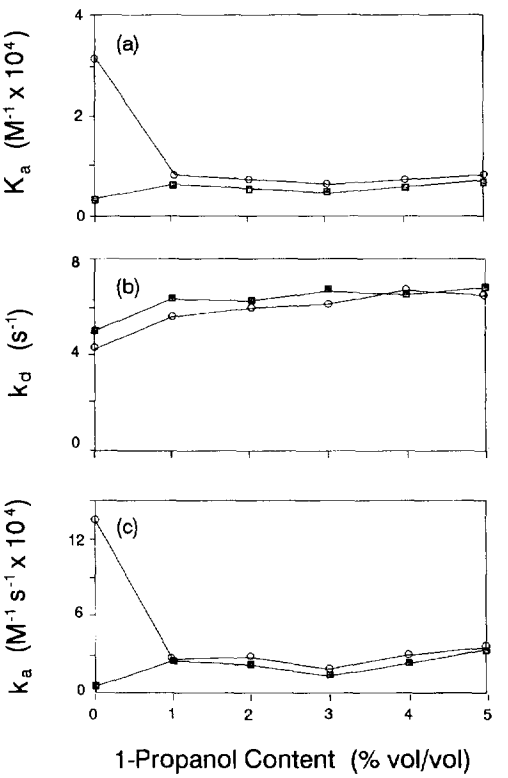

Fig. 6. Effect of mobile phase organic modifier content on the (a) association equilibrium constants, (b) dissociation rate constant, and (c) association rate constants for D-tryptophan (■) and L-tryptophan (○) on an immobilized HSA column.

these results, it was also possible to determine the total change in free energy in going from the reactants to the activated complex ($\Delta G^{\ddagger}$). Furthermore, it was possible to generate energy diagrams for each of these interactions, as shown in Fig. 3b, by combining the data in Table 1 (and related constants determined at 4°C) with previous values reported for the overall change in free energy (ΔG) due to the binding of D- or L-tryptophan to this immobilized HSA support [13].

The $\Delta G^{\ddagger}$ values given in Table 1 and in Fig. 3b for the formation of the activated complex at 37°C are similar for D- and L-tryptophan (i.e., 12.0 versus 10.9 kcal/mol), but there are significant differences in the relative contributions of enthalpy and entropy to $\Delta G^{\ddagger}$ for these two enantiomers. Both D- and L-tryptophan required a net input of energy to overcome the loss of entropy that occurs during the formation of their activated complexes with HSA (i.e., a positive value for $-T\Delta S^{\ddagger}$); however, the change in energy due to entropy was more than two-fold greater for L-tryptophan than for D-tryptophan. Along with this, D-tryptophan had a fairly large positive value for $\Delta H^{\ddagger}$, indicating that more bond breakage than formation occurred for this compound in going from the reactants (i.e., free solute and protein) to the solute–protein activated complex. This could reflect the removal of solvent from D-tryptophan or HSA during the initial stages of the binding process. L-Tryptophan had a negative value for $\Delta H^{\ddagger}$, an unusual feature which suggested that a significant amount of bond formation occurred between this compound and HSA during the early stages of their reaction. This is probably due to long range forces, such as the ionic interactions that are thought to take place between L-tryptophan and

Table 1
Parameters for the temperature dependence of D- and L-tryptophan binding kinetics with immobilized HSA[a]

Compound	$\Delta H^{\ddagger}$ (kcal/mol)	$\Delta S^{\ddagger}$ (cal/mol K)	$-T\Delta S^{\ddagger}$ at 37°C (kcal/mol)	$\Delta G^{\ddagger}$ at 37°C (kcal/mol)
D-Tryptophan	5.5 (±0.9)	−21.1 (±0.4)	6.5 (±0.1)	12.0 (±0.9)
L-Tryptophan	−4.3 (±0.6)	−48.9 (±0.2)	15.2 (±0.1)	10.9 (±0.6)

[a]The numbers in parentheses represent ±1 S.D. All values were determined with data obtained at pH 7.0 in 0.05 *M* potassium phosphate buffer containing no organic modifier.
The numbers given for $\Delta S^{\ddagger}$ were calculated by using one as the value for κ in Eq. (6).
1 cal = 4.184 J.

cationic groups located within the indole site of HSA [18,20,21].

It is useful to compare the free energy diagrams for D- or L-tryptophan and HSA at 4 and 37°C to help to understand how the kinetics of these interactions are affected by temperature. In the case of D-tryptophan, there is a slight increase in the activation barriers for association and dissociation in going from 4 to 37°C, but the greater energy of the reactants at 37°C still gives a net increase in the association and dissociation rates and k_a or k_d, as shown in Fig. 2. In the case of L-tryptophan, an even larger change in the activation barriers occurred with increasing temperature. The data in Fig. 2 indicate that there was still a net increase in the rate of L-tryptophan dissociation despite this higher barrier, thus giving rise to an increase in k_d. However, the extra energy at 37°C for the reactants in the association process (i.e., free L-tryptophan and HSA, plus associated solvent) was apparently insufficient to compensate for the higher barrier, thus resulting in a decrease in k_a. This effect appears to be related to the large change in entropy involved in this particular association process.

Along with temperature, the kinetics between D- or L-tryptophan and HSA were also examined under a range of different mobile phase conditions, including variations in pH, ionic strength and solvent polarity. Previous work with D- and L-tryptophan in zonal elution and frontal analysis studies has shown that these two compounds exhibit very different thermodynamic properties and changes in retention as such mobile phase conditions are altered, with L-tryptophan generally showing the largest effects [4,13]. This is not too surprising considering the proposed nature of binding between HSA and L-tryptophan. For example, it is known that L-tryptophan binds at the indole–benzodiazepine site of HSA in an enthalpy-driven process [13,20,21] that involves several different types of interactions, including non-polar forces between the indole group of L-tryptophan and hydrophobic amino acids (e.g., tyrosine 411) [16,18,20,21] and association of the carboxyl group of L-tryptophan with cationic groups at the end of the binding site [18,20,21]. In contrast, D-tryptophan is thought to interact with a separate region on HSA [4,13] that involves a much looser type of association [33] and a reaction that is predominantly entropy-driven [13].

The effects of changing the pH of the mobile phase on the kinetics of D- and L-tryptophan binding with HSA are illustrated in Fig. 4. As noted earlier [13], both enantiomers had a decrease in K_a in going from a pH value of 7.4 to 4.0, with the largest change being seen for L-tryptophan. For L-tryptophan, the data in Fig. 4 show that the decrease in K_a in going from neutral to acidic pH was due to both a decrease in the rate of dissociation and an increase in the rate of association. These might reflect either changes in the conformation of the binding region or changes in coulombic interactions and/or hydrogen bonding at the binding site [3,21]. For D-tryptophan, the decrease seen in K_a over the same pH range was due predominantly to an increased rate of dissociation. This could also be due to alterations in the conformation of HSA or in some of the interactions between D-tryptophan and the amino acid residues of HSA.

The result of changing the ionic strength of the mobile phase on the kinetics of D- and L-tryptophan is shown in Fig. 5, where the ionic strength was varied by changing the phosphate concentration of the mobile phase. The association equilibrium constant for L-tryptophan shows a large decrease be-

tween 0.0125 and 0.25 *M* phosphate (−74%), along with a smaller decrease in binding strength for D-tryptophan (−10%) under the same conditions [13]. It has been suggested that this decrease in K_a at high phosphate levels may reflect an increased shielding of ionic interactions or a decrease in dipole–dipole interactions between these solutes and HSA [3,13]. Both solutes gave a general increase in the rate of dissociation with increasing phosphate concentration. This is consistent with a weakening of ionic or dipole–dipole interactions. Furthermore, L-tryptophan exhibited a decrease in the association rate constant when going from 0.0125 to 0.067 *M* phosphate. Such behavior fits with a shielding-type effect and appears to account for most of the change in K_a values that was observed for L-tryptophan as a result of variations in the ionic strength.

The effect of varying the polarity of the mobile phase (e.g., 1-propanol content) on the kinetics of tryptophan–HSA binding was the final item examined in this work. The results are summarized in Fig. 6. The K_a data given in Fig. 6a show that the association equilibrium constant for L-tryptophan has a large decrease between 0 to 1% 1-propanol (−79%), followed by much smaller variations between 1-propanol levels of 1 and 5%. For D-tryptophan, a small but significant increase in K_a occurs throughout the entire range of 0 to 5% 1-propanol [13]. According to Fig. 6b–c, the initial decrease in K_a for L-tryptophan between 0 and 1% 1-propanol is almost entirely due to a decrease in the rate of association between this solute and its binding site. Such behavior probably reflects the competition of 1-propanol for the non-polar residues of HSA that take place in binding to L-tryptophan or conformational changes at the indole site of HSA that lead to a decrease in the extent of L-tryptophan binding. Above 1% 1-propanol, D-tryptophan and L-tryptophan show parallel changes not only in their K_a values but also in their values for k_a and k_d. This suggests that the two solutes are either subject to similar changes in reaction entropy under these conditions [13] or that competition by 1-propanol at the indole site causes L-tryptophan to now bind predominantly to the same region and amino acid residues as D-tryptophan.

The data in Figs. 2–6 show that there are many possible ways by which the rate constants, and corresponding plate heights, of HSA columns can be varied to obtain more efficient separations. These include essentially all of the experimental variables that were examined in this study (e.g., temperature, pH, ionic strength and solvent polarity). However, care must be taken to avoid using conditions that also cause a decrease in retention (K_a) or in the observed difference in retention between solutes. The data presented in Figs. 2–6 are useful in that they allow the effects on both retention and efficiency to be examined simultaneously. For example, the results in Fig. 4 indicate that the increase in dissociation rates at lower pH values for D- and L-tryptophan would lead to a narrowing of the solute peaks and a decreased plate height due to stationary phase mass transfer, as noted experimentally in Fig. 1. But although this would appear at first glance to provide a means for obtaining more efficient separations, it must be remembered that there is also a large decrease in K_a over the same pH range that causes a loss in stereoselectivity and retention of these solutes, as shown in Fig. 4a. A similar situation would occur for these solutes when adding 1% or more of 1-propanol to the mobile phase (see Fig. 6). Changing the ionic strength or temperature of the mobile phase for this particular case allows for better control of the separation, since the kinetics can be altered over a wider range of conditions while still allowing a fairly large difference in K_a values to be obtained for D- and L-tryptophan.

An example illustrating the use of such data for optimizing a chiral separation is shown in Fig. 7. In this case, the first set of conditions (Fig. 7a) provided a separation factor that was fairly large (i.e., $\alpha = 1.21$), but the widths of the peaks created significant overlap and produced less than ideal resolution ($R_s = 0.58$). However, based on the trends noted in Figs. 2–6, it was possible to adjust the column conditions in order to improve the efficiency of this separation while maintaining about the same relative difference in retention. In this case, this was done by lowering the pH and raising the ionic strength of the mobile phase slightly, while also increasing the column temperature. This provided about the same separation factor as in Fig. 7a (new $\alpha = 1.25$), but the increase in dissociation rates under the new set of conditions provided narrower peaks that now gave a separation with baseline resolution ($R_s = 1.50$). This example illustrates the need to consider peak widths (or system efficiency) along with differences in

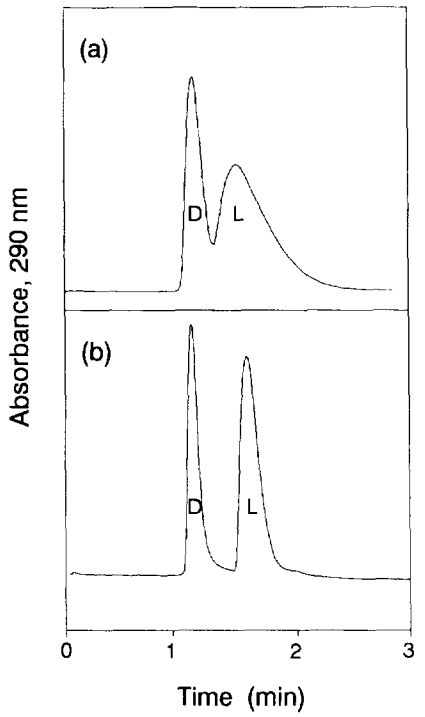

Fig. 7. Separation of D- and L-tryptophan on an immobilized HSA column (a) at pH 7.0 and 10°C in 0.10 *M* phosphate buffer and (b) at pH 6.5 and 37°C in 0.20 *M* phosphate buffer. The flow-rate was 2.0 ml/min.

retention (or separation factors) in the design of protein-based chiral separations. It also illustrates how knowledge of the kinetics and thermodynamics of solute–protein binding, and the role of the mobile phase in controlling these interactions, can be used in optimizing such separation methods.

Acknowledgments

This work was supported by the National Institutes of Health under grant No. GM44931.

References

[1] D.W. Armstrong, Anal. Chem., 59 (1987) 84A.
[2] T.J. Ward, Anal. Chem., 66 (1994) 633A.
[3] S. Allenmark, Chromatographic Enantioseparation: Methods and Applications, Ellis-Horwood, New York, NY, 2nd Ed., 1991.
[4] J. Yang and D.S. Hage, J. Chromatogr., 645 (1993) 241.
[5] B. Loun and D.S. Hage, Anal. Chem., 66 (1994) 3814.
[6] B. Loun and D.S. Hage, Anal. Chem., 68 (1996) 1218.
[7] T.C. Pinkerton, W.J. Howe, E.L. Ulrich, J.P. Comiskey, J. Haginaka, T. Murashima, W.F. Walkenhorst, W.M. Westler and J.L. Markley, Anal. Chem., 67 (1995) 2354.
[8] A. Dugaiczyk, S.W. Law and O.E. Dennison, Proc. Natl. Acad. Sci. USA, 79 (1982) 71.
[9] A. Kaplan and L.L. Szabo, Clinical Chemistry: Interpretation and Techniques, Lea and Febiger, Philadelphia, PA, 1979, Ch. 5.
[10] M.M. Reidenberg and S. Erill (Editors), Drug–Protein Binding, Praeger, New York, NY, 1986.
[11] J.-P. Tillement, G. Houin, R. Zini, S. Urien, E. Albengres, J. Barre, M. Lecomte, P. D'Athis and B. Sebille, Adv. Drug Res., 13 (1984) 59.
[12] W.E. Muller and U. Wollert, Nauyn-Schmiedeberg's Arch. Pharmacol., 288 (1975) 17.
[13] J. Yang and D.S. Hage, J. Chromatogr. A, 725 (1996) 273.
[14] V. Tittelbach and R.K. Gilpin, Anal. Chem., 67 (1995) 44.
[15] C. Lagercrantz, T. Larsson and I. Denfors, Comp. Biochem. Physiol., 69C (1981) 375.
[16] W.E. Müller, K.J. Fehske and S.A.C. Schläfer, in M.M. Reidenberg and S. Erill (Editors), Drug–Protein Binding, Praeger, New York, NY, 1986.
[17] X.M. He and D.C. Carter, Nature, 358 (1992) 209.
[18] D.C. Carter and J.X. Ho, Adv. Protein Chem., 45 (1994) 153.
[19] U. Kragh-Hansen, Pharmacol. Rev., 33 (1981) 17.
[20] R.H. McMenamy and J.L. Oncley, J. Biol. Chem., 233 (1958) 1436.
[21] R.H. McMenamy and R.H. Seder, J. Biol. Chem., 238 (1963) 3241.
[22] R.R. Walters, in I.M. Chaiken (Editor), Analytical Affinity Chromatography, CRC Press, Boca Raton, FL, 1987, Ch. 3.
[23] D.J. Anderson and R.R. Walters, J. Chromatogr., 376 (1986) 69.
[24] J.C. Giddings, Dynamics of Chromatography, Marcel Dekker, New York, NY, 1965.
[25] D.S. Hage, R.R. Walters and H.W. Hethcote, Anal. Chem., 58 (1986) 274.
[26] J.H. Espenson, Chemical Kinetics and Reaction Mechanisms, McGraw-Hill, New York, NY, 1981, Ch. 6.
[27] P.K. Smith, R.I. Krohn, G.T. Hermanson, A.K. Mallia, F.H. Gartner, M.D. Provenzano, E.K. Fujimoto, N.M. Goeke, B.J. Olson and D.C. Klenk, Anal. Biochem., 150 (1985) 76.
[28] E. Grushka, M.N. Myers, P.D. Schettler and J.C. Giddings, Anal. Chem., 41 (1969) 889.
[29] D.J. Anderson and R.R. Walters, J. Chromatogr. Sci., 22 (1984) 353.
[30] T. Whittem and D.C. Ferguson, Endocrinology, 127 (1990) 2190.
[31] J.A. Jansen, Acta Pharmacol. Toxicol., 41 (1977) 401.
[32] R.G. Reed, J. Biol. Chem., 252 (1971) 7483.
[33] G. Uccello-Barretta, C. Bertucci, E. Domenici and P. Salvadori, J. Am. Chem. Soc., 113 (1991) 7017.